Supporting Information

Unraveling the interactions of reductants and reaction path over Cu-ZSM-5 for model coal-gas-SCR via transient reaction study

Jie Cheng, Ruinian Xu, Ning Liu, Chengna Dai, Gangqiang Yu, Ning Wang and Biaohua Chen*

Faculty of Environment and Life, Beijing University of Technology, Beijing 100124, China

*Corresponding Authors: Ruinian Xu

xuruinian@bjut.edu.cn (R. Xu)

S1. XRD results

S2. TPD results

S3. TPSR results

S4. *In situ* DRIFTS results

Fig. S1. XRD spectra of Cu based catalyst with different topology structure.

Fig. S2. H_2 signal (a), CO signal (b), CH_4 signal (c) of Cu-ZSM-5 catalyst at different adsorption conditions.

Fig. S3. MS signals of Cu-ZSM-5 catalyst at different reaction conditions.

Fig. S4. *In situ* DRIFTS spectra of (a) H_2, (b) CO, (c) CH_4, (d) CO + H_2, (e) CH_4 + H_2, (f) CH_4 + CO, and (g) CH_4 +CO + H_2 reacted with pre-adsorbed NO + O_2 on Cu-ZSM-5 catalyst at 250^{o}C as a function of time.

Fig. S5. *In situ* DRIFTS spectra of (a) NO + H_2 + O_2, (b) NO + CO + O_2, (c) NO + CH_4 + O_2, (d) NO + CO + H_2 + O_2, (e) NO + CH_4 + H_2 + O_2, (f) NO + CH_4 + CO + O_2 and (g) NO + CH_4 + CO + H_2 + O_2 on Cu-ZSM-5 catalyst at 250 ^{o}C as a function of time.

Fig. S6. *In situ* DRIFTS spectra of (a) NO + CO + H_2 + O_2, (b) stop CO + H_2, (c) NO + CH_4 + H_2 + O_2, (d) stop CH_4 + H_2, (e) NO + CH_4 + CO + O_2, (f) stop CH_4 + CO (e) NO + CH_4 + CO + H_2 + O_2 and (f) stop CH_4 + CO + H_2 on Cu-ZSM-5 catalyst at 250 ^{o}C as a function of time.

Fig. S7. *In situ* DRIFTS spectra in the range of 2400-2000 cm^{-1} (a) stop H_2, (b) stop CO, (c) stop CH_4, (d) stop CO + H_2, (e) stop CH_4 + H_2, (f) stop CH_4 + CO and (g) stop CH_4 + CO + H_2 on Cu-ZSM-5 catalyst at 250 ^{o}C as a function of time.

Fig. S8. *In situ* DRIFTS spectra of (a) NO + H_2 + O_2, (b) stop H_2, (c) NO + CO + O_2, (d) stop CO, (e) NO + CH_4 + O_2 and (f) stop CH_4 on Cu-ZSM-5 catalyst at 250 ^{o}C as a function of time.

Fig. S9. *In situ* DRIFTS spectra on Cu-ZSM-5 catalyst at 250 °C under different reaction condition.

Fig. S10. *In situ* DRIFTS spectra on Cu-ZSM-5 catalyst at 350 °C under different reaction condition.

Table S1. Observed species in the reaction process as identified by IR.

Table S2. Reaction steps of various SCR reactions.

S1. XRD results

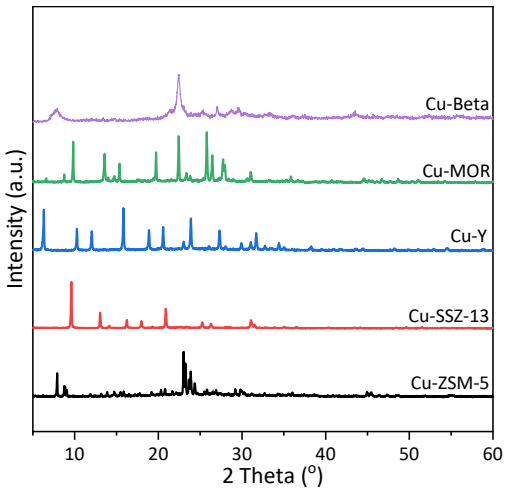

Fig. S1. XRD spectra of Cu based catalyst with different topology structure.

As shown in **Fig. S1**, five kinds of zeolite catalyst with different topology structure exhibit complete diffraction peak according to the database of IZA [1], which indicated that the modification process did not deteriorate zeolite structure. In addition, the characteristic signals of CuO species (2θ=35.5 and 38.8°) are not observed in all patterns, suggesting that CuO species were highly dispersed on the zeolite.

S2. TPD results

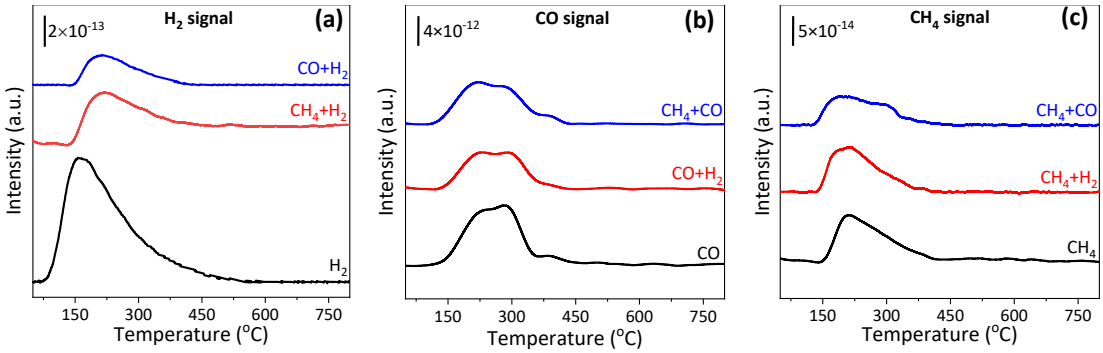

Fig. S2. H_2 signal (a), CO signal (b), CH_4 signal (c) of Cu-ZSM-5 catalyst at different adsorption conditions.

In order to explore the competitive adsorption between reductants, the H_2, CO,

and CH_4 signal at different adsorption conditions were monitored. As shown in **Fig. S2**, after introducing CO + H_2 and CH_4 + H_2 for co-adsorption, the intensity of H_2 signal greatly decreased, which indicated that CO and CH_4 were regarded as an inhibitor for the H_2 adsorption. Moreover, the H_2 signal in the flow of CO + H_2 is weaker than that of CH_4 + H_2, indicating that the inhibition effect of CO is stronger than CH_4 which may be due to the strong adsorption ability of CO. As for CO and CH_4 adsorption, the introduction of external reducing agent has little effect on its adsorption.

S3. TPSR results

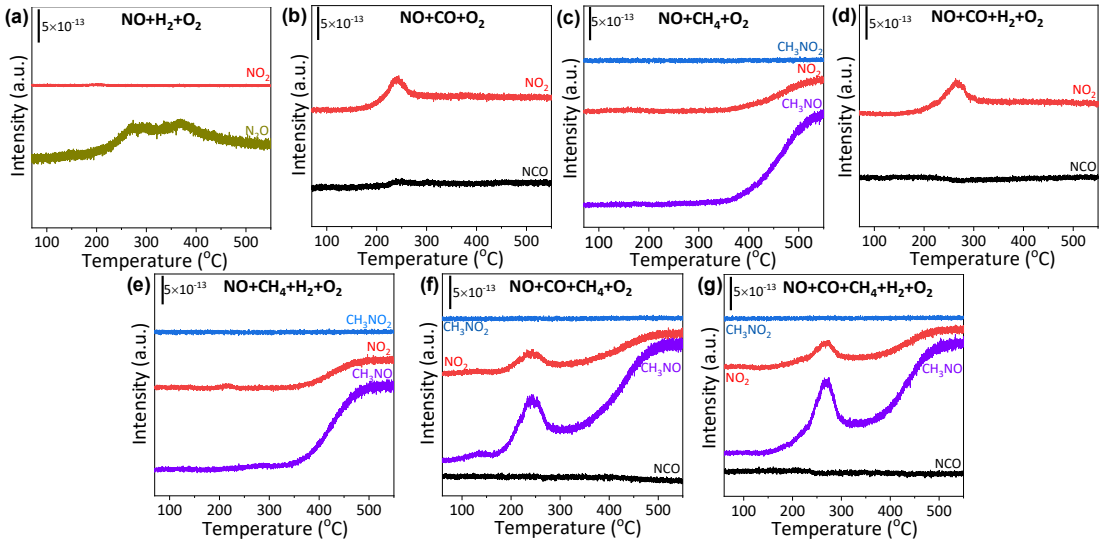

Fig. S3. MS signals of Cu-ZSM-5 catalyst at different reaction conditions.

S4. *In situ* DRIFTS results

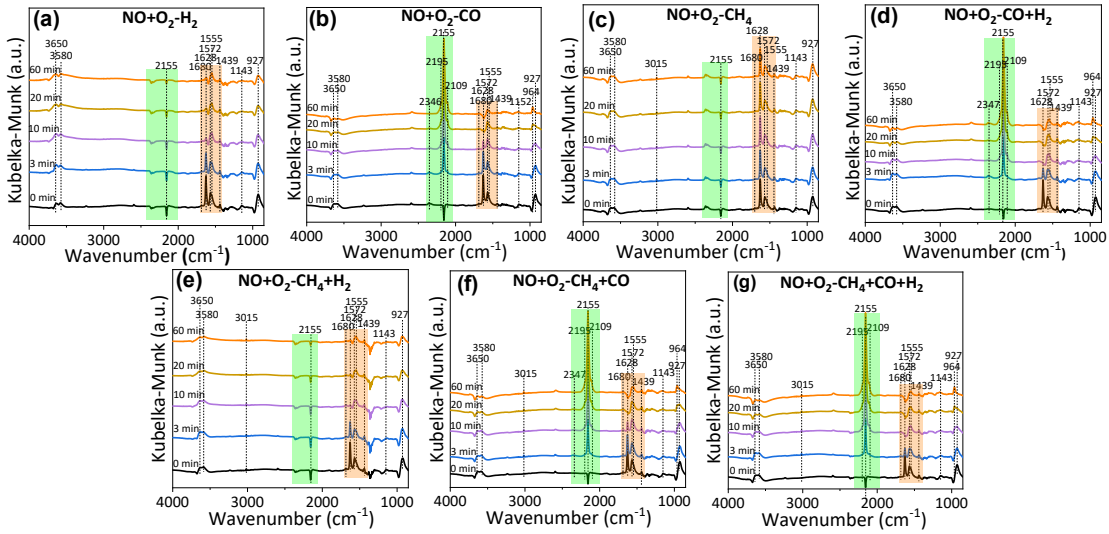

Fig. S4. *In situ* DRIFTS spectra of (a) H_2, (b) CO, (c) CH_4, (d) CO + H_2, (e) CH_4 + H_2, (f) CH_4 + CO, and (g) CH_4 + CO + H_2 reacted with pre-adsorbed NO + O_2 on Cu-ZSM-5 catalyst at 250 °C as a function of time.

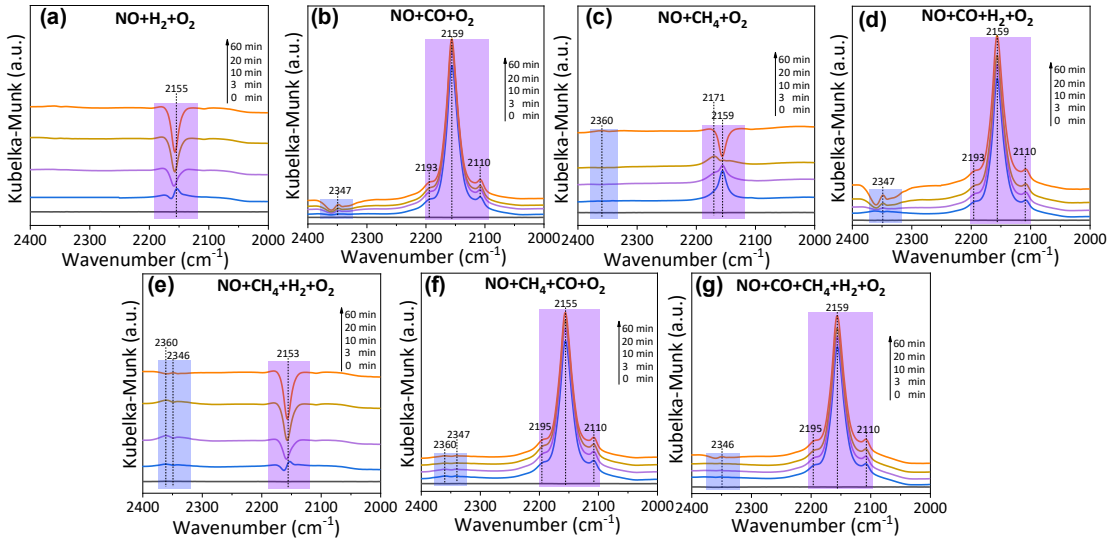

Fig. S5. *In situ* DRIFTS spectra of (a) NO + H_2 + O_2, (b) NO + CO + O_2, (c) NO + CH_4 + O_2, (d) NO + CO + H_2 + O_2, (e) NO + CH_4 + H_2 + O_2, (f) NO + CH_4 + CO + O_2 and (g) NO + CH_4 + CO + H_2 + O_2 on Cu-ZSM-5 catalyst at 250 °C as a function of time.

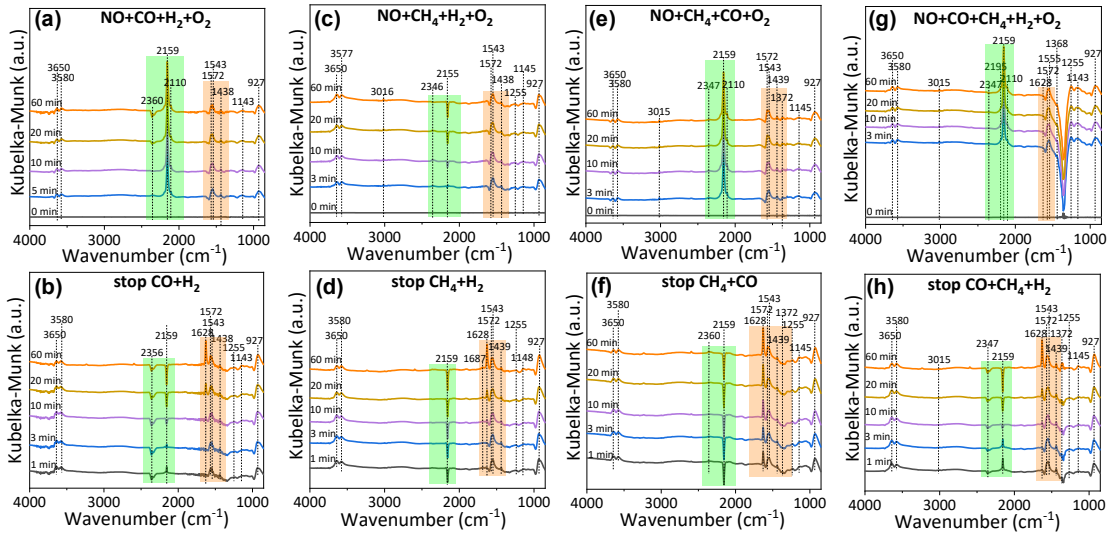

Fig. S6. *In situ* DRIFTS spectra of (a) NO + CO + H_2 + O_2, (b) stop CO + H_2, (c) NO + CH_4 + H_2 + O_2, (d) stop CH_4 + H_2, (e) NO + CH_4 + CO + O_2, (f) stop CH_4 + CO (e) NO + CH_4 + CO + H_2 + O_2 and (f) stop CH_4 + CO + H_2 on Cu-ZSM-5 catalyst at 250 ^oC as a function of time.

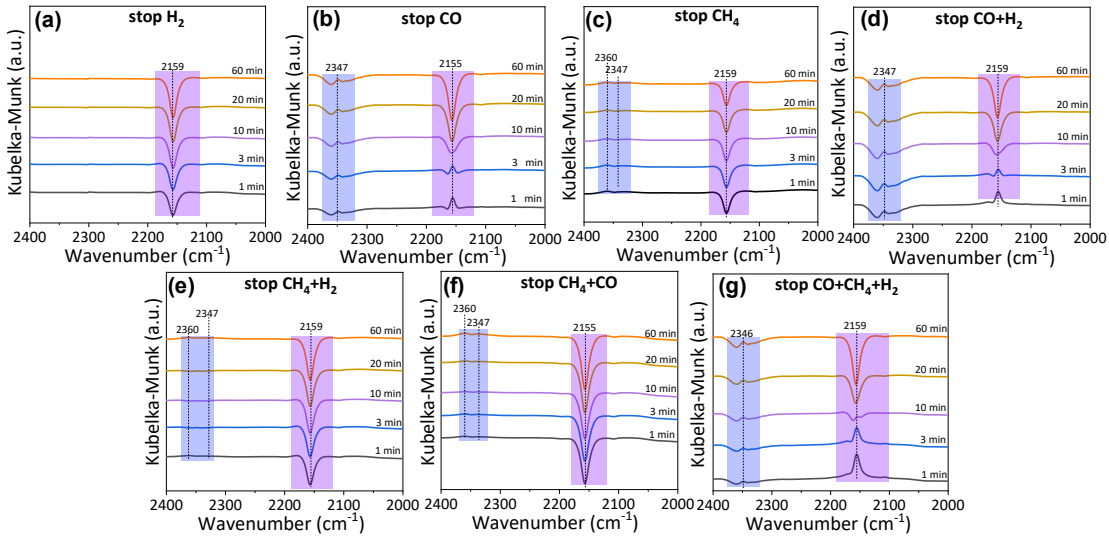

Fig. S7. *In situ* DRIFTS spectra of (a) stop H_2, (b) stop CO, (c) stop CH_4, (d) stop CO + H_2, (e) stop CH_4 + H_2, (f) stop CH_4 + CO and (g) stop CH_4 + CO + H_2 on Cu-ZSM-5 catalyst at 250 ^oC as a function of time.

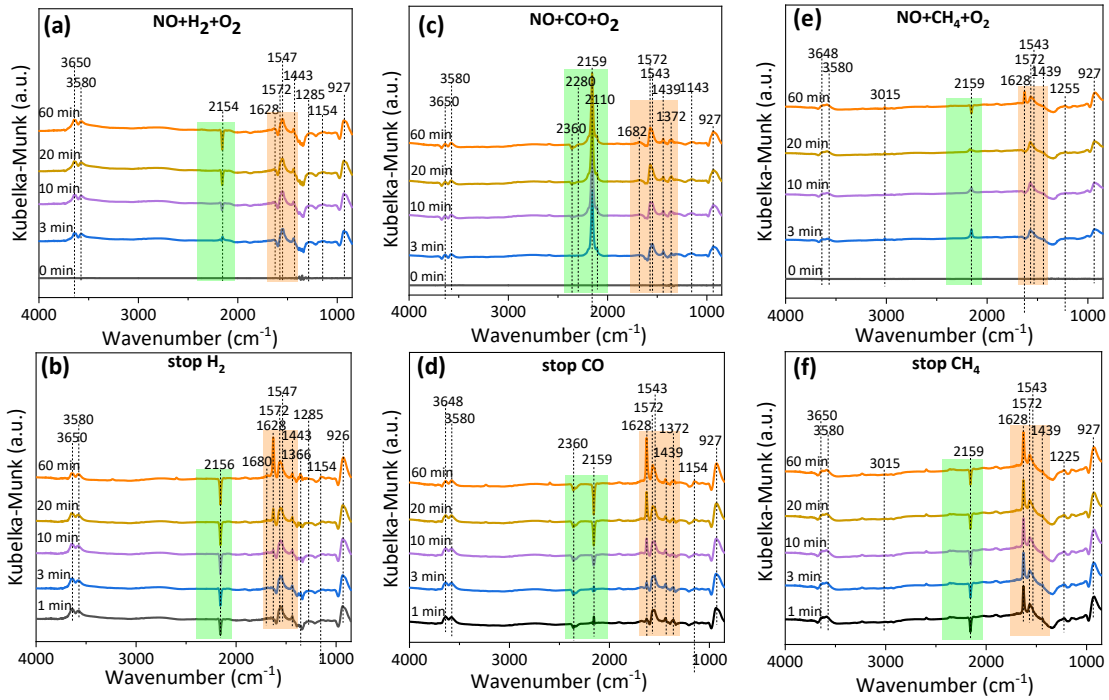

Fig. S8. *In situ* DRIFTS spectra of (a) NO + H_2 + O_2, (b) stop H_2, (c) NO + CO + O_2, (d) stop CO, (e) NO + CH_4 + O_2 and (f) stop CH_4 on Cu-ZSM-5 catalyst at 250 ^oC as a function of time.

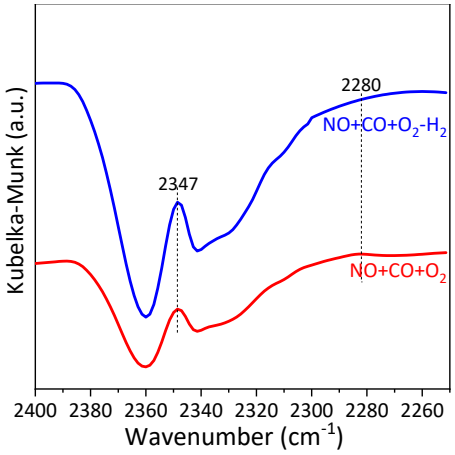

Fig. S9. *In situ* DRIFTS spectra on Cu-ZSM-5 catalyst at 250 °C under different reaction conditions.

In order to investigate the effect of H_2 on the generation of intermediate species in CO-SCR process, the catalyst first was exposed to the flow of NO + CO + O_2 for reaction, and then H_2 was introduced in the reaction. As shown in **Fig. S9**, when exposed the catalyst to NO + CO + O_2 reaction system, a band at 2280 cm^{-1} was appeared in spectra, which could be ascribed to NCO species, which is an important intermediate species in CO-SCR reaction [2]. However, after introducing H_2 for reaction, the intensity of this band vanished, which means that addition of H_2 could reduce the amount of NCO species, thus the presence of H_2 may change the reaction route in CO-SCR process.

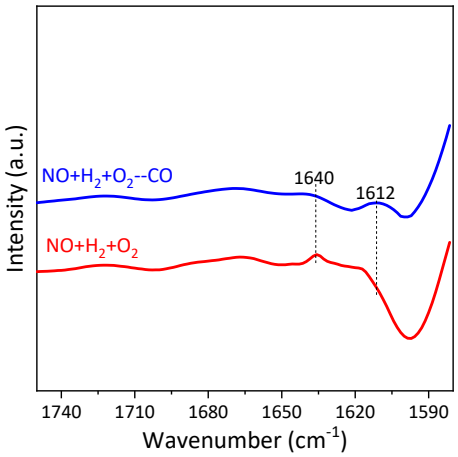

Fig. S10. *In situ* DRIFTS spectra on Cu-ZSM-5 catalyst at 350 °C under different reaction conditions.

To investigate the inhibitory effect of CO on the generation of NH_x species from H_2, the catalyst was first exposed to the flow of NO + H_2 + O_2 for reaction, and then CO was added into the reaction. As shown in **Fig. S10**, a peak at 1640 cm^{-1} attributed to NH_4^+ species appeared after introduction of H_2 [3], which indicated that NH_4^+ species was formed in the SCR process. However, after injecting CO, the intensity of 1640 cm^{-1} weakened to almost disappear, indicating CO could have an obvious inhibition on the formation of NH_x species.

Table S1. Observed species in the reaction process as identified by IR.

Wavenumber (cm^{-1})	Species and mode	Ref.
1143	Adsorbed NO	4
1255	Bridged nitrates	4
1439	Nitrites	5
2155	NO^+ species	6
964	Bidentate carbonates	7
1372	Monodentate carbonate	8
2109/2155	$Cu^+(CO)$ carbonyl	9, 10
2195	$Cu^+(CO)_2$ carbonyl	11
2346/2360	Adsorbed CO_2	12
1285	Coordinated NH_3	13
3015	Adsorbed CH_4	14
3580	Si-OH-Al	15
3650	Cu-OH	15

Table S2. Reaction steps of various SCR reactions.

Reaction type	Reaction steps	No.
NO adsorption and nitrate formation	$NO + * \rightarrow NO*$	R1
	$O_2 + * \rightarrow O_2*$	R2
	$NO* + *\rightarrow N* + O*$	R3
	$O_2* + *\rightarrow O* + O*$	R4
	$N* + N* \rightarrow N_2 + 2*$	R5
	$NO* + N* \rightarrow N_2O + 2*$	R6
	$NO* + O_2* \rightarrow NO_2* + O*$	R7
	$NO* + O_2{}^{-}* \rightarrow NO_3{}^{-}* + *$	R8
	$N_2O* \rightarrow N_2 + O*$	R9
H_2-SCR	$H_2 + * \rightarrow H_2*$	Ra1
	$H_2* \rightarrow 2H*$	Ra2
	$N* + H* \rightarrow NH* + *$	Ra3
	$NH* + H* \rightarrow NH_2* + *$	Ra4
	$NH_2* + H* \rightarrow NH_3* + *$	Ra5
	$O* + H* \rightarrow OH* + *$	Ra6
	$OH* + H* \rightarrow H_2O + 2*$	Ra7
	$NO_2* + H_2* \rightarrow ONH* + OH*$	Ra8
	$ONH* + NO* + H* \rightarrow N_2 + H_2O + O* + 2*$	Ra9
	$ONH* + NO* + H* \rightarrow N_2O* + H_2O + 2*$	Ra10
	$4NH_3 + 4NO + 2O_2 \rightarrow 4N_2 + 6H_2O$	Ra11
	$2NH_3 + NO + NO_2 \rightarrow 2N_2 + 3H_2O$	Ra12
CO-SCR	$CO + * \rightarrow CO*$	Rb1
	$N* + CO* \rightarrow NCO* +*$	Rb2
	$NO_2* + CO* \rightarrow NCO* + O_2*$	Rb3
	$CO* + 2NO_2* \rightarrow N_2 + CO_2 + 3O*$	Rb4
	$NCO* + NO* \rightarrow N_2 + CO_2 + 2*$	Rb5
	$CO* + O* \rightarrow CO_2 + 2*$	Rb6
	$2NCO* + 3H_2O \rightarrow 2NH_3 + 2CO_2 + O*$	Rb7
	$NCO* + NO_2* \rightarrow N_2 + CO_2 + * + O*$	Rb8
CH_4-SCR	$CH_4* + O* \rightarrow CH_3* + OH*$	Rc1
	$CH_3* + O* \rightarrow CH_2* + OH*$	Rc2
	$NO* + CH_3* \rightarrow CH_3NO* + *$	Rc3
	$4CH_3NO + 2NO + 4O_2 \rightarrow 3N_2 + 6H_2O + 4CO_2$	Rc4
	$CH_4 + 2O_2 \rightarrow CO_2 + 2H_2O$	Rc5
	$2NO + CH_4+ O_2 \rightarrow N_2 + CO_2 + 2H_2O$	Rc6

References

1. Database of Zeolite Structures, http://www.iza-structure.org/databases/).
2. Y. H. Yeom, B. Wen, W. M. H. Sachtler and E. Weitz, *The Journal of Physical Chemistry B*, 2004, **108**, 5386-5404.
3. D. Meng, W. Zhan, Y. Guo, Y. Guo, L. Wang and G. Lu, *ACS Catal.*, 2015, **5**, 5973-5983.
4. Q. Wang, H. Xu, W. Huang, Z. Pan and H. Zhou, *J. Hazard. Mater.*, 2019, **364**, 499-508.
5. S. Lai, D. Meng, W. Zhan, Y. Guo, Y. Guo, Z. Zhang and G. Lu, *RSC Adv.*, 2015, **5**, 90235-90244.
6. H.-Y. Chen, M. Kollar, Z. Wei, F. Gao, Y. Wang, J. Szanyi and C. H. F. Peden, *Catal. Today*, 2019, **320**, 61-71.
7. K. I. Hadjiivanov and G. N. Vayssilov, *Advances in Catalysis*, 2002, **47**, 307-511.
8. H. L. Huynh, J. Zhu, G. Zhang, Y. Shen, W. M. Tucho, Y. Ding and Z. Yu, *J. Catal.*, 2020, **392**, 266-277.
9. H. I. Hamoud, V. Valtchev and M. Daturi, *Appl. Catal. B: Environ.*, 2019, **250**, 419-428.
10. H. Zhou, Z. Huang, C. Sun, F. Qin, D. Xiong, W. Shen and H. Xu, *Appl. Catal. B: Environ.*, 2012, **125**, 492-498.
11. V. L. Sushkevich, D. Palagin, M. Ranocchiari and J. A. van Bokhoven, *Science*, 2017, **356**, 523.
12. S. M. Fehr and I. Krossing, *ChemCatChem*, 2020, **12**, 2622-2629.
13. G. Qi, R. Yang and F. Rinaldi, *J. Catal.*, 2006, **237**, 381-392.
14. Y. Shi, J. Pu, L. Gao and S. Shan, *Chem. Eng. J.*, 2021, **403**, 126394.
15. J. Song, Y. Wang, E. D. Walter, N. M. Washton, D. Mei, L. Kovarik, M. H. Engelhard, S. Prodinger, Y. Wang, C. H. F. Peden and F. Gao, *ACS Catal.*, 2017, **7**, 8214-8227.